metals

MDPI

Article

Microstructure and Mechanical Properties of TC4 Titanium Alloy at the Temperature of 77K

Yuetao Zhao [1,2], Xuewen Li [1,*] and Wenbin Fang [2]

[1] Key Laboratory for Light-Weight Materials, Nanjing University of Technology, Nanjing 210003, China
[2] School of Materials Science and Chemical Engineering, Harbin University of Science and Technology, Harbin 150040, China
* Correspondence: lixuewen2000@163.com

Abstract: Titanium alloy has the advantages of low thermal conductivity, a small expansion coefficient and being non-magnetic, making it an ideal low-temperature structural material. In this paper, the typical TC4 titanium alloy in industrial titanium alloy is selected as the research object. The microstructure deformation law and mechanical behavior of TC4 titanium alloy at liquid nitrogen temperature are mainly investigated, and compared with the microstructure and properties at room temperature. The macroscopic and microscopic deformation mechanism of the simultaneous increase in elongation and hardening index of titanium alloy at low temperature is revealed, which provides a basic basis for the low-temperature deformation mechanism and strengthening and toughening design of titanium alloy. Based on the uniaxial tensile tests at room temperature (298 K) and low temperature (77 K), the effects of low temperature on the yield strength, elongation, tensile strength and work hardening curve of titanium alloy were compared and analyzed. The strength/plasticity synergistic improvement of TC4 titanium alloy under low-temperature deformation was found. At low temperature, the yield strength, tensile strength and elongation of TC4 titanium alloy are improved compared with room temperature. The tensile strength increases from 847.93 MPa at 298 K to 1318.70 MPa at 77 K, and the elongation increases from 21.8% at 298 K to 24.9% at 77 K. The grain morphology, grain orientation, dislocation density and fracture morphology of titanium alloy under room temperature and low-temperature tensile conditions were studied by SEM and EBSD. The results of fracture morphology characterization at room temperature and low temperature show that TC4 titanium alloy exhibits ductile fracture characteristics and a large number of dimples are formed on the fracture surface. The dimple depth at low temperature is shallower than that at room temperature and the overall surface is more flat. Compared with room temperature deformation, the deformation process of TC4 titanium alloy in a low-temperature environment produces stronger dislocation pile-up and forms a large number of twins, but the grain rotation is more significant, which effectively alleviates the stress concentration and delays the initiation and propagation of cracks at grain boundaries.

Keywords: TC4 titanium alloy; low temperature; mechanical property; microstructure evolution

check for updates

Citation: Zhao, Y.; Li, X.; Fang, W. Microstructure and Mechanical Properties of TC4 Titanium Alloy at the Temperature of 77K. *Metals* **2023**, *13*, 1086. https://doi.org/10.3390/met13061086

Academic Editors: Antonio Mateo and Maciej Motyka

Received: 3 April 2023
Revised: 30 May 2023
Accepted: 6 June 2023
Published: 8 June 2023

Copyright: © 2023 by the authors. Licensee MDPI, Basel, Switzerland. This article is an open access article distributed under the terms and conditions of the Creative Commons Attribution (CC BY) license (https://creativecommons.org/licenses/by/4.0/).

1. Introduction

Titanium alloy has the advantages of high strength, high toughness and low thermal conductivity [1,2]. Titanium alloys are widely used in aerospace and other fields. Excellent corrosion resistance makes titanium alloy materials favored in the field of navigation and the chemical industry. Good biocompatibility is widely used in bioengineering and medical fields [3,4]. The advantages of excellent thermal conductivity and low expansion coefficient make titanium a suitable new low-temperature material. The deep-sea temperature is 1 °C, and the highest temperature in the Antarctic region is only about −22 °C. Under the radiation of the sun, the equilibrium temperature of the surface in the spacecraft will reach

−90~310 °C, and the lowest can reach −190 °C [5]. Titanium alloys are also mainly used in these low-temperature environments such as space and deep sea.

With the development of aerospace technology, the application of titanium alloy at low temperature is also significantly improved. The structural components in spacecraft require further improvement of the low-temperature performance required by the equipment environment. The alloy must meet the requirements of sufficient strength and toughness at low temperatures, excellent thermal properties and good machinability because of the complex shape of the structural parts [6]. At low temperature, titanium alloy has higher yield strength than traditional alloy, which is more than three times of stainless steel, and the density is only half of stainless steel [7]. As a typical α + β titanium alloy, TC4 is the earliest developed and successfully applied titanium alloy material, and it is also the most widely used titanium alloy so far [8]. Low-temperature titanium alloys with excellent service performance, such as TA17ELI, TC4ELI, CT20, LT700, etc., have been developed [9,10]. In the field of low-temperature titanium alloys in the United States, for low-temperature titanium alloys α + β type titanium alloy TC4ELI for some conduits and liquid hydrogen catheters in the Apollo program has been widely used and achieved good results [11–13]. Compared with developed countries such as the United States and Russia, China started late in the field of low-temperature titanium alloy research and development, and the technology research and development of C, H, O and other interstitial elements and the reduction of aluminum content are relatively backward. With spaceflight development, China researched low-temperature titanium alloys [14]. CT20 is the first low-temperature titanium alloy with independent property rights in China. It can be used at a very low temperature of 20 K and has excellent formability. At present, it has been applied to a spacecraft cryogenic pipeline. At the same time, Du Yu, Zhang Zhong, Fan Chengliang and others found that the occurrence of twinning behavior is the main deformation mechanism in low-temperature environments [15–19].

TC4 titanium alloy is a (α + β) two-phase titanium alloy, where α belongs to the close-packed hexagonal structure and β belongs to the body-centered cubic structure. [20]. The two-phase designs are different, and the slip will start from the α-phase grains, which are influenced by β and gradually expand to the surrounding β-transformed tissue [21]. The important deformation mechanism of Ti-6Al-4V at low temperatures is twinning [22–24]. Microstructural changes in TC4 at low temperatures can impact the aircraft life of space engines. The aim of this work is to test the mechanical properties of TC4 titanium alloy at low temperature. It can not only explain the correlation of the micro-deformation mechanism of TC4 titanium alloy during the quasi-static mechanical properties test at low temperature, but also help to increase the understanding of the low-temperature failure behavior of TC4 titanium alloy and the accumulation of performance data. It provides some help for the application of titanium alloys in low-temperature environments such as aviation, ships, and aerospace. At the same time, it provides a basis for the progress of traditional titanium alloys and the development of low-temperature titanium alloys. It has important practical research value and corresponding engineering application background.

2. Materials and Methods

The experimental material is TC4 titanium alloy aviation forging and its nominal composition is Ti-6Al-4V (wt.%). The initial observation of the original structure showed that the microstructure of TC4 titanium alloy was equiaxed, as shown in Figure 1a. The average diameter of equiaxed primary α grains is 18 μm, the diameter of secondary α grains is 7 μm, and the diameter of interstitial β grains is 0.8 μm. Reference [25] pointed out that secondary α appeared after processing at a relatively low temperature in the α/β region. According to Image-Pro Plus 6.0 statistics, α accounted for 93.22% and β accounted for 6.78%.

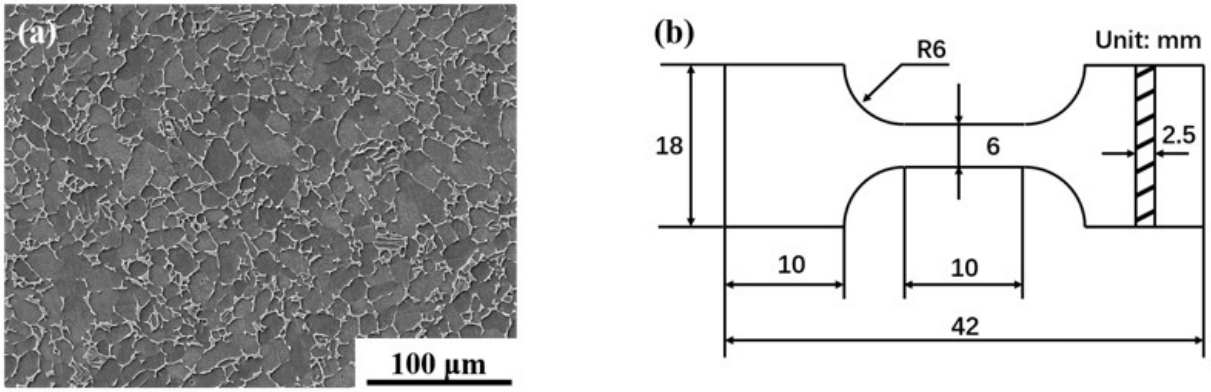


Figure 1. The original microstructure morphology and tensile size of TC4 titanium alloy: (**a**) TC4 titanium alloy original structure (**b**) tensile specimen size.

The tensile specimen of TC4 titanium alloy is shown in Figure 1b. MTS C45.105 full temperature field mechanical properties testing machine was used to test the mechanical properties at room temperature and low temperature. The low-temperature test method is as follows: In the low-temperature tensile test, the whole tensile process was carried out in an incubator with liquid nitrogen, and the tensile rate was 5×10^{-4}/s. The sample is fixed by a hook–hang structure, and the sample is installed in the mechanical property test machine. In order to ensure the firmness of the sample, the sample is preloaded by adjusting the moving end beam of the stretching machine. The cooling method is to pour the liquid nitrogen solution into the incubator, let the sample soak in the liquid nitrogen solution, and stand for 30 min in the heat preservation state. In the process of dumping liquid nitrogen, due to the physical factors of the principle of thermal expansion and cold contraction, in order to ensure that the internal structure of the sample is not destroyed, the data should be observed and collected at all times in the process of dumping liquid nitrogen and heat preservation, and the beam should be adjusted appropriately. In the tensile test at room temperature, the TC4 titanium alloy sample was completed without liquid nitrogen immersion. The samples in each state were subjected to three tensile tests to ensure the authenticity of the mechanical properties.

In order to study the microstructure evolution during the deformation process at different temperatures, the microstructure of the tensile specimens after fracture was characterized. During the tensile process, the material enters the plastic deformation stage after passing through the elastic deformation stage. According to the principle of constant volume in the plastic deformation stage, the accurate width and thickness of the deformed sample are used for careful quantitative calculation.

The surface of the sample was subjected to mechanical grinding and electrolytic polishing. The composition of the electrolytic polishing solution is 5% perchloric acid ($HCLO_4$) + 35% n-butanol (CH_3 (CH_2) 3OH) + 60% methanol (CH_3OH). The parameters of electrolytic polishing are as follows: −20 °C, constant current 0.8 A, voltage about 40 V, polishing time 50 s, cathode stainless steel, anode sample, electrode spacing about 2 cm, magnetic stirring. The TESCAN S8000 GMH field emission electron microscope was used. The SEM acceleration voltage was 20 keV, the current was 20 nA, and the working distance of the objective lens was 20 mm. The EBSD working lens distance was 13 mm.

3. Results and Discussion

3.1. Microstructure of TC4 Titanium Alloy

The forged TC4 titanium alloy structure is analyzed and characterized, as shown in Figure 2. The microstructure of TC4 titanium alloy was observed. EBSD technique was used to show the grain orientation distribution, phase distribution, grain size distribution and XRD phase analysis of TC4 titanium alloy. From the grain orientation distribution, as shown in Figure 2a, it can be seen that there are some unique characteristics of the forging

state and some weak macro zone effects [26]. It can be seen from the phase distribution diagram, as shown in Figure 2b, TC4 titanium alloy is mainly composed of α phase and β phase. Among them, one can find that the β phase content is shallow, mainly distributed in the α grain boundary of the grain. At the same time, the statistics of grains are also carried out, as shown in Figure 2c. According to the statistics, it can be concluded from the grain statistical distribution that the grain size of TC4 titanium alloy is relatively uniform and has the characteristics of an equiaxed structure. As shown in Figure 2d, XRD analysis shows that the material is composed of α-Ti phase and β-Ti phase, and the results are consistent with the phase analysis diagram in EBSD analysis data.

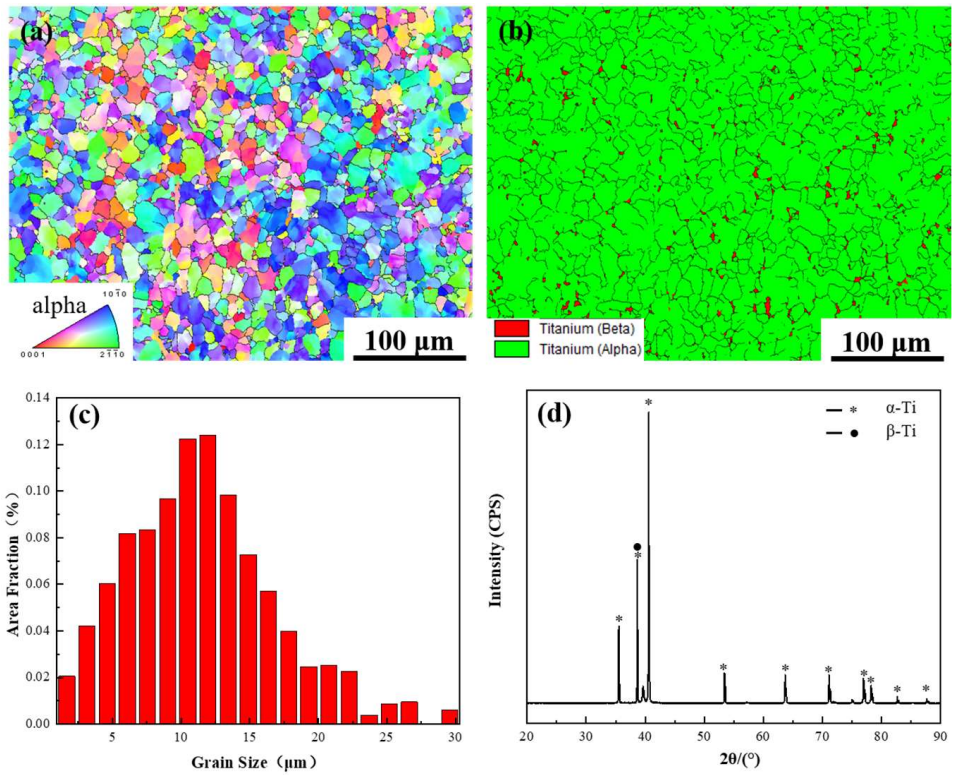


Figure 2. Microstructure and phase distribution of TC4 titanium alloy: (**a**) orientation distribution; (**b**) phase distribution diagram; (**c**) Grain size drawing; (**d**) XRD results.

3.2. Analysis of Mechanical Properties of TC4 Titanium Alloy

The mechanical curves of TC4 titanium alloy at room temperature and low temperature are shown in Figure 3. It is found that the material is mainly divided into four stages during the stretching process. One stage is the elastic stage. At this stage, the tensile stress increases linearly with the rapid growth of strain. When the stress exceeds the yield strength, it enters the second stage, the yield stage. Because there is no obvious yield strength point in this curve, the stress value that produces 0.2% residual deformation is the yield limit [27]. When entering the yield stage, the linear relationship between stress and strain is destroyed, and the stress tends to be uniform as the tension progresses. As the stress continues to increase beyond the yield limit, it enters the third stage, the strengthening stage. At this stage, obvious and uniform plastic deformation occurs, the strain of the sample increases, and the stress value will inevitably increase. At this stage, dislocation slips and produces mutual entanglement and accumulation. This phenomenon is called work hardening. As the strain continues to increase, the alloy enters the final stage, the fracture stage. When cracks appear inside the alloy, due to the decrease in the bearing area, the overall deformation strengthening effect is weakened, which shows that the mechanical property curve shows a downward trend, and the material curve shows ductile fracture.

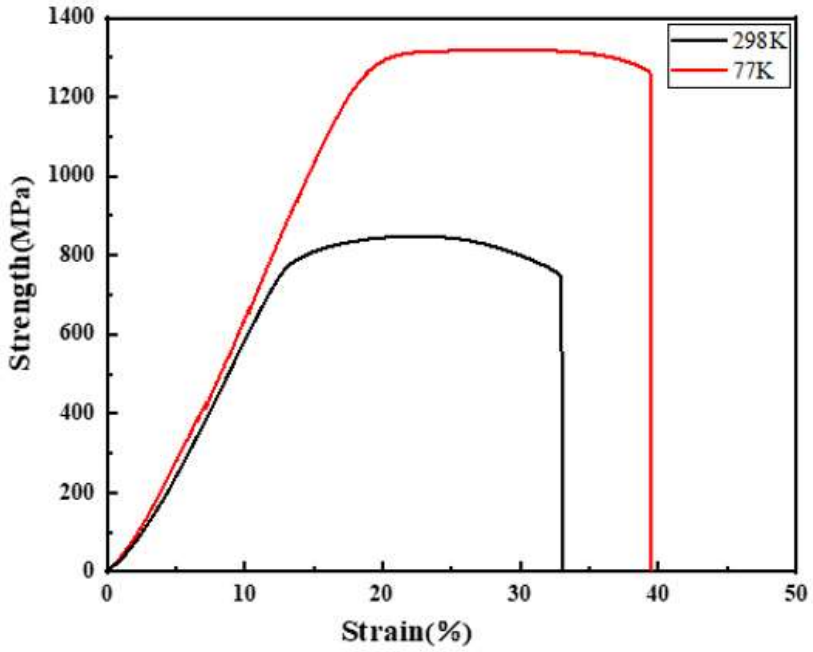


Figure 3. Stress–strain curve of titanium alloy at room temperature and low temperature.

Table 1 lists the yield strength (YS), tensile strength (UTS), and elongation after the break of materials at room temperature and low temperature (ε). When the temperature is reduced to 77 K, the yield strength, tensile strength and elongation of the sample are significantly higher than those at 298 K. It shows that the change of internal structure of TC4 titanium alloy at low temperatures is beneficial to the increase in mechanical properties.

Table 1. Test temperature is 77 K and 298 K mechanical property results.

Temperature (K)	Yield Strength (MPa)	Ultimate Tensile Strength (MPa)	Elongation after a Break (%)
298	761.2	847.9	21.8
77	1120.1	1318.7	24.9

3.3. Quantitative Calculation of TC4 Titanium Alloy Non-Deformation

The microstructure of the material is closely related to its mechanical properties. The study of the deformation behavior of the material is inseparable from the change of the microstructure. Next, the stress state and grain orientation distribution of TC4 titanium alloy at room temperature and low temperature are compared and explored. The fracture of the gauge section was removed by using TC4 titanium alloy stretched at room temperature and low temperature. During the tensile process, the material entered the plastic deformation stage after the elastic deformation stage. According to the principle of constant volume of the material in the plastic deformation stage, the accurate width and thickness of the deformed sample were used for careful quantitative calculation, as shown in Figure 4. In the stress–strain curve of the room temperature sample, the yield strength is the position where the strain is at 13%, so the shooting area is searched at the beginning of the yield point, and the strain is reached at 13% and 25%, respectively. The yield strength obtained from the stress–strain curve of the low-temperature specimen is the position where the strain is at 17%. The corresponding fracture of the low-temperature tensile specimen is selected at the position corresponding to 17% and 25% for calibration analysis. In the calculation process, the error of the corresponding position to the mark point is controlled at about 0.03 mm, and the corresponding force is about 5N.

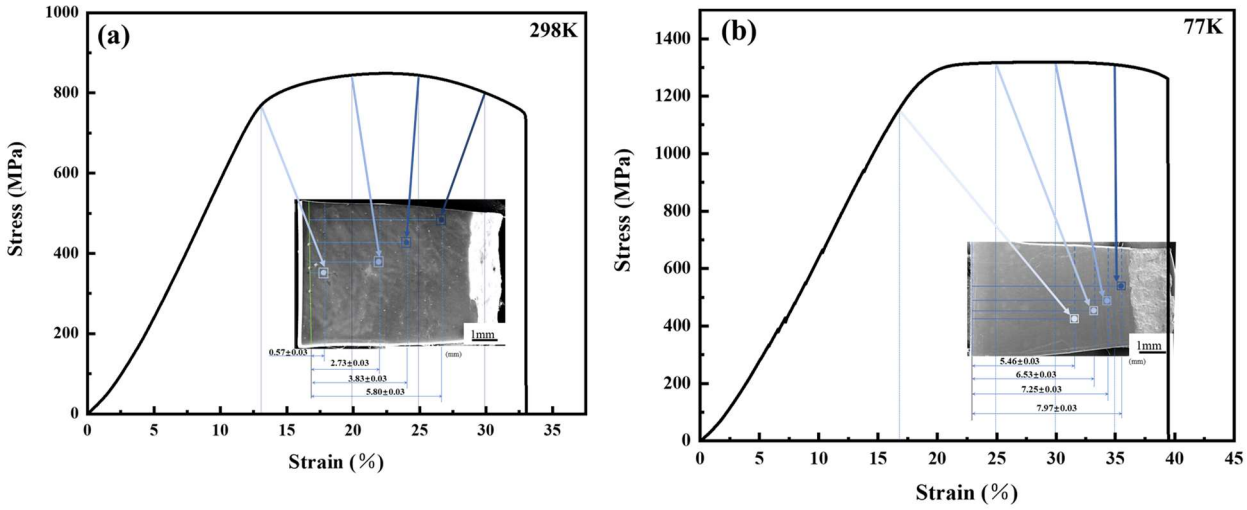


Figure 4. Schematic diagram of different deformations corresponding to different positions: (**a**) 298 K, (**b**) 77 K.

3.4. Microstructure Evolution of Mechanical Properties of TC4 Titanium Alloy

According to the mechanical curve, TC4 titanium alloy has excellent tensile mechanical properties at low temperature, which shows that the deformation of material and structure is closely related to the stretching. In this study, according to the influence of the tensile curve, firstly, the microstructure analysis of TC4 titanium alloy samples was compared at the yield stage of room temperature and low temperature. The IPF map of TC4 titanium alloy at room temperature and low temperature is shown in Figure 5a,c. The twins of TC4 titanium alloy appear first in the yield stage of tension at low temperature.

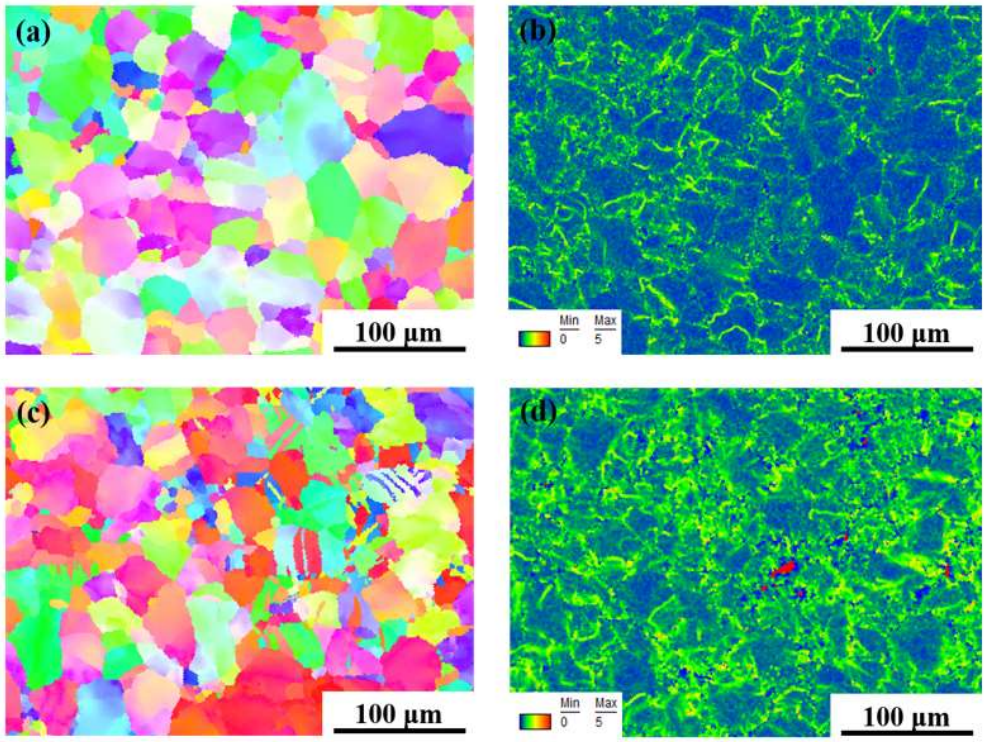


Figure 5. Microstructure analysis of yield strength stage of TC4 titanium alloy at room temperature and low temperature: (**a**,**c**) orientation distribution, (**b**,**d**) Orientation difference distribution diagram.

The grain size shows the deformation behavior of grains in different degrees, directly affecting the dislocation movement and interaction during the deformation process [25].

Figure 5b,d show the distribution of orientation difference. The calculation principle collects the difference between the average orientation of different points and the grain, which describes the degree of grain deformation. As shown in the figure, it is easy to see the secondary formation with a relatively small grain size α. The orientation difference of the region is higher than that of the primary crystal with a rather large grain size α area. The deformation near the grains in the primary α region is larger than that inside [27]. The stress increases step by step from inside to outside. By observing Figure 5b,d, it is found that work hardening is closely related to the current environment. Because the dislocation density is relatively low at room temperature, the effect of work hardening ability is not obvious. With the decrease in temperature, the dislocation density increases, the dislocation accumulation is severe, and the flow stress is significantly higher than that of TC4 titanium alloy deformed at room temperature. When the critical shear stress of the activated dislocation is greater than or equal to the twin shear, mechanical twins begin to appear. From the grain orientation Figure 5c, it is not difficult to find that there are a large number of deformation twins in some larger grains. In general, the material will produce corresponding stress concentration when the dislocation slip is difficult to activate, and twinning is more likely to occur in such a region. The formation of twin boundaries refines the grains and hinders the further slip of dislocations, thus strengthening the material.

The TC4 titanium alloy is based on the premise of different temperatures at room temperature and low temperature. In the orientation distribution Figure 6a,c, it is found that the dislocation density of TC4 titanium alloy at low temperature is more intense than that at room temperature, partly caused by a large number of twins, which is consistent with the analysis of the orientation distribution map. At low temperatures, more slip systems are activated in TC4 titanium alloy, resulting in more internal stress, which provides conditions for the generation of a large number of twins. Twins also provide more interaction between dislocations and twin boundaries for stress. It is found that twinning occurs in large-sized α grains. The complementary way of plastic deformation usually produces twins when crystal dislocations are difficult to slide, which provides more opportunities for dislocation slip to change grain orientation [28]. Therefore, while the twins provide plastic deformation, the corresponding twin boundaries are generated to hinder the interaction slip and further strengthen the material. Twins in large-sized α grains can indicate that large-sized primary α grains provide more strain than small-sized secondary α grains under the same strain conditions. It is found that the number of mechanical twins in the orientation distribution diagram at low temperature (Figure 6c) is as high as 80% higher than that at room temperature (Figure 6a). The main effects of twins can be summarized as follows: (i) crystal reorientation, adjusting the activation trend of the slip system; (ii) Grain refinement leads to the strengthening of the Hall–Petch relationship and the resulting yield; and (iii) the formation of immobile dislocations through the interaction of twin boundaries and dislocations, which contributes to work hardening.

In the corresponding grain orientation difference Figure 6b,d, it is found that from the grain orientation difference, it can be seen that compared with room temperature, the dislocation density at low temperature is more intense, the strain concentration is more obvious, and the TC4 titanium alloy starts more slip systems at low temperature.

Generally, KAM (Kernel Average Misorientation) analyzes the average orientation difference between EBSD scanning points with increased strain. It mainly reflects the lattice deformation caused by strain accumulation [29]. Figure 6b,d show the KAM statistical distribution of samples with 25% elongation at room and low temperatures. It can be seen from the results that the KAM value at both temperatures reached about 5°. The main reason is that the amount of drawing deformation at room temperature and low temperature is the same, so the degree of deformation accumulation has no decisive effect on the lattice deformation. However, comparing the KAM values at two temperatures can find that the distribution angle of KAM at room temperature is relatively high compared with that at low temperatures. This shows that the strain accumulation caused by dislocation movement at low temperatures is less than at room temperature. In other words, a large part of tensile

deformation at low temperatures is caused by dislocation movement at the grain boundary, consistent with the previous expression.

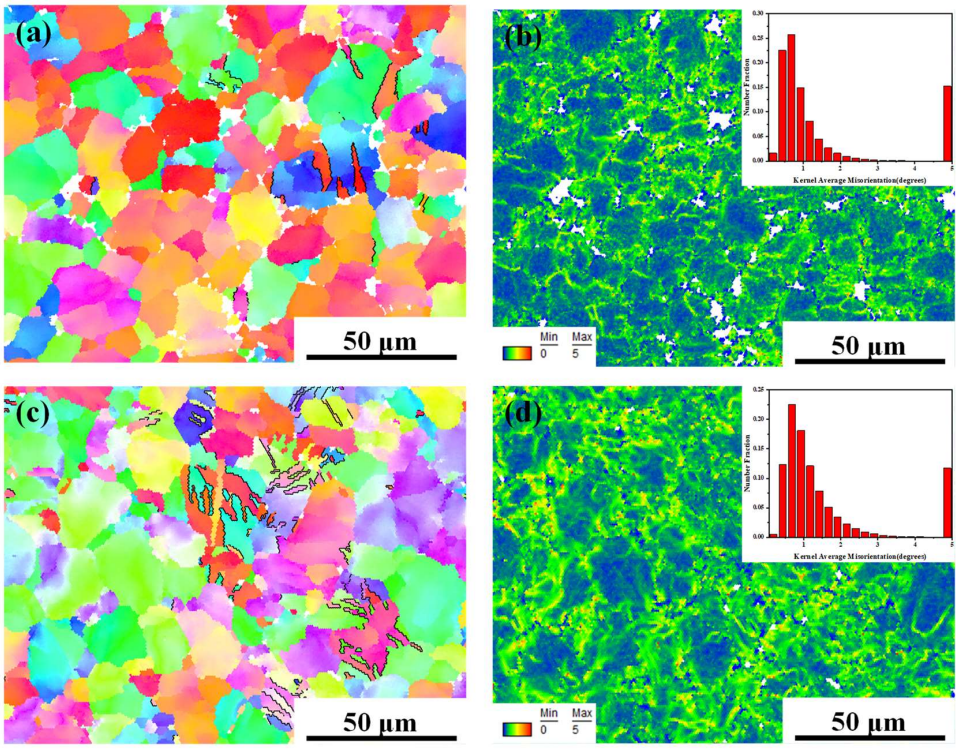


Figure 6. Microstructure of TC4 titanium alloy with 25% strain variable: (**a**) IPF at room temperature (**b**) KAM and statistical distribution plot at room temperature (**c**) IPF at low temperatures (**d**) KAM and statistical distribution plot of low temperatures.

3.5. TC4 Titanium Alloy Fracture Morphology Analysis

Scanning electron microscopy (SEM) was used to analyze the microstructure of the front and side fractures of TC4 titanium alloy tensile specimens at room temperature and low temperature at different temperatures at quasi-static tensile rate. The scanning results are shown in Figure 7.

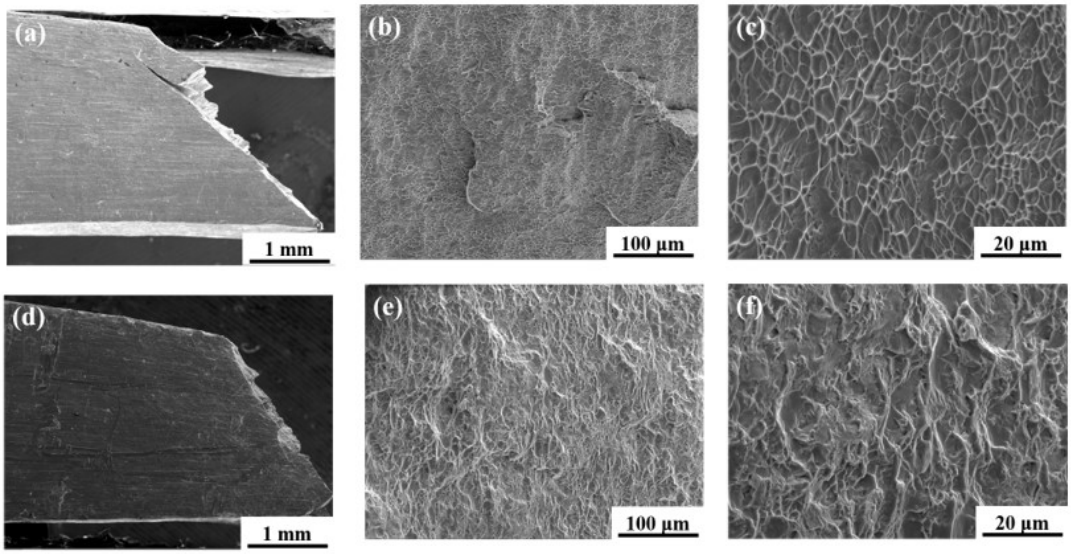


Figure 7. TC4 titanium alloy fracture at different temperatures: (**a**–**c**) low temperature; (**d**–**f**) Room temperature.

The micro-fracture mechanism can be divided into brittle fracture, cleavage fracture or quasi-cleavage fracture, ductile fracture, intergranular fracture, and fatigue fracture. In Figure 7a,d, it is found that both the low temperature and room temperature side fractures have 45° shear fractures, and the fracture behavior is initially determined to be a ductile fracture. Liu Zhidan [30] studied the fracture characteristics of Ti-6Al-4V at different temperatures and found that the fracture form from room temperature to 77 K is ductile. Next, from the front of the fracture, Figure 7b,e represent the fracture morphology in an extensive range, and Figure 7c,f represent the fracture morphology in a small degree. In Figure 7b,c of the cryogenic sample, it can be found from the normal fracture that the plane is relatively smooth, composed of some small dimples, and there are some smooth small facets, showing the characteristics of cleavage fracture. It can also be found that the edge part is composed of a cleavage surface. The deep pits are composed of elongated dimples at high magnification. Figure 7e,f of the sample at room temperature can be relatively flush when observing the large area of the front fracture. The fracture features of equiaxed dimples are found in the small field of view in Figure 7f. The small ligament fossa is in the middle of the large fossa, and the inside of the fossa has a river-like slip line. The standard to the edge of the fracture has a cut edge, elongated shallow fossa, cleavage planes [31], and torn edges. At room temperature, the fracture begins from the microporous aggregation type of the central part to the final cleavage fracture. Overall, the port socket is more uniform, flatter, smaller in diameter, and has a more specific directionality at low temperatures than at room temperature.

4. Conclusions

In this study, TC4 titanium alloy was used as the research object. The microstructures of different deformations near the fracture of tensile specimens at different temperatures of 77 K and 298 K were analyzed. The relationship between mechanical properties and microstructure evolution was explored, and the mechanism of its change was revealed. EBSD technique was used to investigate the initial microstructure and tensile properties of TC4 titanium alloy under uniaxial stress tensile test at room temperature and low temperature. The following conclusions were obtained:

1. After low-temperature treatment, the tensile strength of TC4 alloy at room temperature is 847.9 MPa and the engineering strain is 33.1% at the strain rate of 5×10^{-4} s^{-1}. The tensile strength is 1318.7 MPa and the engineering strain is 39.5% at low temperature. The strength and toughness are in an increasing state at low temperature.
2. The grains of TC4 titanium alloy are broken and refined during the tensile process. With the increase in strain, the local strain will first concentrate in the secondary α grains and then crack, and the stress concentration position will shift to complete fracture. Under the same yield stage, the stress concentration area of titanium alloy in low-temperature deformation environment is more, and twinning behavior is more likely to occur.
3. The micro-fractures of TC4 titanium alloy at room temperature and low temperature show ductile fracture. The size of dimples is equiaxed. The number of dimples at low temperature is more than that at room temperature. The depth of dimples at low temperature is shallower and the overall performance is more even.

Author Contributions: Conceptualization, X.L.; investigation, Y.Z.; writing—original draft preparation, Y.Z.; writing—review and editing, X.L. and W.F.; funding acquisition, X.L. All authors have read and agreed to the published version of the manuscript.

Funding: This research was funded by the National Key R&D Program of China (No.2020YFA0405900), the National Natural Science Foundation of China (No.52271104), and the Natural Science Foundation of Heilongjiang Province of China (No.YQ2020E030).

Institutional Review Board Statement: Not applicable.

Informed Consent Statement: Not applicable.

Data Availability Statement: Not applicable.

Acknowledgments: The authors would like to acknowledge the financial support provide by the National Key R&D Program of China (No.2020YFA0405900), the National Natural Science Foundation of China (No.52271104), and the Natural Science Foundation of Heilongjiang Province of China (No.YQ2020E030).

Conflicts of Interest: The authors declare no conflict of interest.

References

1. Wu, C.; Zhou, Y.J.; Liu, B. Experimental and simulated investigation of the deformation behavior and microstructural evolution of Ti6554 titanium alloy during an electropulsing-assisted microtension process. *Mater. Sci. Eng. A* **2022**, *838*, 142745. [CrossRef]
2. Wang, D.; Dong, H.; Ma, Y.; Li, P.; Wu, B.; Huang, L.; Zhang, L.; Li, J. Microstructure and mechanical properties of TC4 titanium alloy and 316L stainless steel joint by MIG welding with mortise structure. *Weld. Int.* **2022**, *36*, 732–743. [CrossRef]
3. Zhang, Y.; Li, M.; Jiang, K.; Wang, H.; Qu, P.; Wang, H.; Zhu, L. Constitutive Behavior of Titanium Alloy with Dual-Phase Microstructures: Experiments and Modeling. *J. Appl. Mech.* **2023**, *90*, 071009. [CrossRef]
4. Miao, K.; Huang, M.; Xia, Y.; Wu, H.; Liu, Q.; Fan, G. Unexpected de-twinning of strongly-textured Ti mediated by local stress. *J. Mater. Sci. Technol.* **2022**, *125*, 231–237. [CrossRef]
5. Qiu, Y.; Yang, H.; Tong, L.; Wang, L. Research Progress of Cryogenic Materials for Storage and Transportation of Liquid Hydrogen. *Metals* **2021**, *11*, 1101. [CrossRef]
6. Jin, L.; Yang, Y.-F.; Li, R.-Z.; Cui, Y.-W.; Jamil, M.; Li, L. Study on Springback Straightening after Bending of the U-Section of TC4 Material under High-Temperature Conditions. *Materials* **2020**, *13*, 1895. [CrossRef]
7. Mukhopadhyay, M.; Kundu, P.K.; Das, S. Experimental investigation on enhancing grindability using alkaline-based fluid for grinding Ti-6Al-4V. *Mater. Manuf. Process.* **2018**, *33*, 1775–1781. [CrossRef]
8. Chen, W.; Liu, X.; Bu, H.; Wang, F.; Luo, J. Effect of scanning mode on temperature field and interface morphology of laser joining between CFRTP and TC4 titanium alloy. *Int. J. Adv. Manuf. Technol.* **2022**, *123*, 2057–2072. [CrossRef]
9. Omura, H. Application and Manufacturing Technologies of Titanium Alloys for Aircraft Industry(2). *Titan. Jpn.* **2012**, *60*, 289–294.
10. Lei, L.; Zhu, Q.; Zhao, Q.; Yang, M.; Yang, W.; Zeng, W.; Zhao, Y. Low-temperature impact toughness and deformation mechanism of CT20 titanium alloy. *Mater. Charact.* **2023**, *195*, 112504. [CrossRef]
11. Rui, Z.L.; Feng, C.; Long, J.; Cao, Y.Q. Research Status and Development of Titanium Alloy Drill Pipes. *Mater. Sci. Forum* **2019**, *944*, 903–909.
12. Zherebtsov, S.V.; Dyakonov, G.S.; Salem, A.A.; Sokolenko, V.I.; Salishchev, G.A.; Semiatin, S.L. Formation of nanostructures in commercial-purity titanium via cryorolling. *Acta Mater.* **2013**, *61*, 1167–1178. [CrossRef]
13. Liu, T.K.; Wu, G.L.; Liu, C.K.; Nie, Z.H.; Ungar, T.; Ren, Y.; Wang, Y.D. Interface coherency strain relaxation due to plastic deformation in single crystal Ni-base superalloys. *Mater. Sci. Eng. A* **2013**, *568*, 83–87. [CrossRef]
14. Choi, J.H.; Lee, S.J.; Choi, D.H. Tolerance Optimization for Mechanisms with Lubricated Joints. *Multibody Syst. Dyn.* **1998**, *2*, 145–168. [CrossRef]
15. Zhao, Y.; Yang, G. Some Titanium Alloys Developed by NIN and Their Industrial Manufacture. *Titan. Ind. Prog.* **2006**, *6*, 65–70.
16. Zhao, Y.-q.; Zhou, L. Current research situation of titanium alloys in China. *Mater. Res. Appl.* **2005**, *15*, 82–91.
17. Huang, C.; Ge, P.; Zhao, Y.; Xin, S.; Zeng, W. Research Progress in Titanium Alloys at Cryogenic Temperatures. *Rare Met. Mater. Eng.* **2016**, *45*, 254–260.
18. Azmirruddin Ahmad, M.; Jabir, M.; Johari, N.; Ibrahim, R.; Hamidi, N. The effect of impurities elements on titanium alloy (Ti-6Al-4V) MIM sintered part properties. *AIP Conf. Proc.* **2017**, *1901*, 40007.
19. Yang, W.; Ji, W.; Zhou, Z.; Xu, J. Analysis of Deformation Behavior and Microstructure Changes for α/β Titanium Alloy at Elevated Temperature. *Met. Open Access Metall. J.* **2021**, *11*, 303. [CrossRef]
20. Ouchi, C.; Iizumi, H.; Mitao, S. Effects of ultra-high purification and addition of interstitial elements on properties of pure titanium and titanium alloy. *Mater. Sci. Eng. A* **1998**, *243*, 186–195. [CrossRef]
21. Zhang, W.; Chai, D.; Ran, G.; Zhou, J. Study on microstructure and tensile properties of in situ fiber reinforced aluminum matrix composites. *Mater. Sci. Eng. A Struct. Mater. Prop. Misrostruct. Process.* **2008**, *476*, 157–161. [CrossRef]
22. Prakash, D.L.; Ding, R.; Moat, R.; Jones, I.; Withers, P.; da Fonseca, J.Q.; Preuss, M. Deformation twinning in Ti-6Al-4 V during low strain rate deformation to moderate strains at room temperature. *Mater. Sci. Eng. A* **2010**, *527*, 5734–5744. [CrossRef]
23. Castany, P.; Pettinari-Sturmel, F.; Crestou, J.; Douin, J.; Coujou, A. Experimental study of dislocation mobility in a Ti–6Al–4V alloy. *Acta Mater.* **2007**, *55*, 6284–6291. [CrossRef]
24. Castany, P.; Pettinari-Sturmel, F.; Douin, J.; Coujou, A. In situ transmission electron microscopy deformation of the titanium alloy Ti-6Al-4V: Interface behaviour. *Mater. Sci. Eng. A Struct. Mater. Prop. Microstruct. Process.* **2008**, *483–484*, 719–722. [CrossRef]
25. Sun, Y. Corrosion Behavior of Ta-10W Coatings on CP-Ti and TC4 Substrates. *J. Mater. Eng. Perform.* **2019**, *28*, 4152–4162. [CrossRef]
26. Zheng, L. The variation of microstructures, textures and mechanical properties from edge to center in cross section of Ti6242s titanium alloy. *Vac. Technol. Appl. Ion Phys. Int. J. Abstr. Serv. Vac. Sci. Technol.* **2019**, *160*, 81–88. [CrossRef]

27. Garza-Ramos, M.; Estupian-Lopez, F.H.; Gaona-Tiburcio, C.; Beltrán-Novelo, L.; Almeraya-Calderón, F. Electrochemical Behavior of Ti6Al4V Alloy Used in Dental Implants Immersed in Streptococcus gordonii and Fusobacterium nucleatum Solutions. *Materials* **2020**, *13*, 4185. [CrossRef]
28. Lechun, X.; Liqiang, W.; Kuaishe, W.; Guilin, Y.; Yuanfei, F.; Di, Z.; Weijie, L.; Lin, H.; Chang, Z.L. TEM characterization on microstructure of Ti–6Al–4V/Ag nanocomposite formed by friction stir processing. *Materialia* **2018**, *3*, 139–144.
29. Gottstein, M. Variant selection of primary, secondary and tertiary twins in a deformed Mg alloy. *Acta Mater.* **2012**, *60*, 2043–2053.
30. Peng, X.; Guo, H.; Qin, C.; Shi, Z.; Zhao, Z. Isothermal Beta Grain Growth Kinetics of TC4-DT Titanium Alloy under Two Different Prior Processing Conditions: Deformed vs. Undeformed. *Rare Met. Mater. Eng.* **2014**, *43*, 1855–1861. [CrossRef]
31. Zhang, G.; Luo, J.; Zheng, G.; Bai, Z.; Cao, L.; Mao, H. Is the 0.2%-Strain-Offset Approach Appropriate for Calculating the Yield Stress of Cortical Bone? *Ann. Biomed. Eng.* **2021**, *49*, 1747–1760. [CrossRef] [PubMed]

Disclaimer/Publisher's Note: The statements, opinions and data contained in all publications are solely those of the individual author(s) and contributor(s) and not of MDPI and/or the editor(s). MDPI and/or the editor(s) disclaim responsibility for any injury to people or property resulting from any ideas, methods, instructions or products referred to in the content.